Chaotic motion of a passive space object during its contactless transportation by ion beam

V.S. Aslanov[1], A.S. Ledkov[1]

[1]Samara National Research University, Moskovskoe Shosse 34A, Samara, Russia, 443086

Abstract. Contactless transportation of passive objects by an active spacecraft is a promising direction in modern space technology. The study considers plane motion of a passive space object of a cylindrical shape relative its center of mass under the influence of an ion beam created by the active spacecraft's electrodynamic engine. The aim of the work is to study the passive object attitude dynamics during its ion beam transportation. A mathematical model describing the motion of the mechanical system was obtained using the second-order Lagrange equations. A simplified equation describing the perturbed motion of the object in an elliptical orbit was obtained. Bifurcation diagrams showing the influence of the orbit height and the position of the object's center of mass on the type and position of the equilibrium points were constructed. Using the Poincare sections and the spectrum of Lyapunov exponents, it was shown that a chaotic layer exists in the vicinity of the separatrices of the unperturbed system. The chaos can lead to the transition of the object from the oscillation mode to the rotation mode, which will affect the magnitude of the ion forces imparted by the ion beam to the object, and the duration of the transportation mission.

1. Introduction

The space debris removal is one of the most important tasks of modern astronautics. Currently in orbit there are a large number of non-functioning satellites and rocket stages, which mutual collision can lead to the formation of a cloud of space debris, and make large areas of outer space inaccessible for practical use. Reviews of the space debris problem and possible ways of it removal by active spacecraft are given in papers [1-3]. One of the promising directions among space debris cleaning systems currently under development is ion-based contactless transportation systems. There are several interesting researches on the study of the orbital motion of a passive object under the influence of an ion beam. Part of the work is devoted to the physics of the plasma plume expansion and its interaction with the surface of a body [4-7].The methods for calculating the forces and moments imparted by a height-velocity stream of particles to the body can be found in papers [8-10]. Part of the work is devoted to studying the motion of the center of mass of space debris during its transportation by ion beam and developing an active spacecraft relative position control laws [11-14]. Article [15] is devoted to the selection of contactless space debris removal system parameters. In these works, the motion of the transported object relative to its center of mass and the effect of this motion on the magnitude of the ion beam forces and moments are not taken into account. It was shown in articles [10] that the motion of an object relative to the center of mass has a significant effect on the efficiency of ion transport. The article [16] proposes the laws of ion beam control that provide stabilization of the angular motion of a cylindrical passive object in the most favourable position for its ion transportation.

An interesting approach to a rocket stage detumbling using contactless ion interaction is described in the article [17].

The aim of the work is to study the space debris attitude dynamics during its ion beam transportation. This article explores the attitude motion of space debris of a cylindrical shape under the influence of the ion beam. The choice of this form is due to the fact that many space debris objects have such a shape. In particular, the cylindrical bodies are the upper stages of rockets, for example Cosmos or Arian, and satellites, for example Parus (USSR) or Telestar 301 (USA).

It is assumed that the cylinder center of mass lies on the axis of its symmetry. The planar motion of the system under the influence of gravitational and ionic forces and moments is considered in this study. An active spacecraft creating an ion beam is considered as a mass point.

2. Mathematical model

The state of a mechanical system consisting of a space debris object and an active spacecraft can be described by five generalized coordinates (figure 1): the position vector module r, the true anomaly angle ν, the deflection angle of the space debris axis from the position vector θ, the coordinates of the active spacecraft in Local-vertical/local-horizontal reference frame (LVLH) x and y. The origin of this frame is at the center of the mass of the space debris (point B on figure 1). The axis Bx_o is directed along the position vector. The axis By_o is perpendicular to Bx_o, and it is directed towards the space debris orbital motion. The active spacecraft is equipped with an ion engine that creates an ion beam and a propulsion system that compensates the operation of the ion engine and allowing control the spacecraft motion. The resulting thrust of the active spacecraft engines is shown in figure 1 by the vector $\mathbf{P}$. The effect of the ion beam on space debris can be represented in the form of two mutually perpendicular forces F_x and F_y, which are directed along the axes of the body coordinate system $Bx_b y_b$ associated with space debris, and the torque L_z relative to the center of mass B, which vector is perpendicular to the plane of the figure 1.

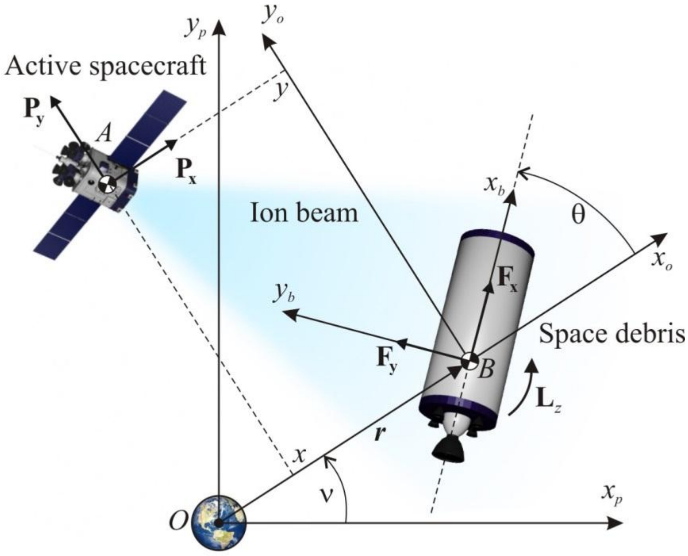

Figure 1. Considered mechanical system.

Lagrange function of the considered mechanical system can be written in the form

$$L = \frac{m_A V_A^2}{2} + \frac{m_B V_B^2}{2} + \frac{I_z(\dot{\nu} + \dot{\theta})^2}{2} + \frac{\mu m_A}{r_A} + \frac{\mu m_B}{r} + \frac{\mu(I_x + I_y + I_z)}{2r^3} - \frac{3\mu(I_x \cos^2\theta + I_y \sin^2\theta + I_z)}{2r^3}, \quad (1)$$

where m_A is the mass of the spacecraft, m_B is the mass of the space debris, I_x, I_y, and I_z are the principle moments of inertia of the space debris, μ is the gravitational constant of the Earth,

$r_A = \sqrt{(r+x)^2 + y^2}$ is the distance between the active spacecraft and the center of the Earth, V_A is the velocity of the spacecraft, V_B is the velocity of the space debris:

$$V_A^2 = (r+x)^2\dot{\nu}^2 + y^2\dot{\nu}^2 + 2((r+x)\dot{y} - y(\dot{r}+\dot{x}))\dot{\nu} + (\dot{r}+\dot{x})^2 + \dot{y}^2 + y^2\dot{\nu}^2, \qquad V_B^2 = r^2\dot{\nu}^2 + \dot{r}^2. \quad (2)$$

The equations of motion of a mechanical system can be written in the form of Lagrange equations of the second kind

$$\frac{d}{dt}\frac{\partial L}{\partial \dot{q}_i} - \frac{\partial L}{\partial q_i} = Q_i, \quad (3)$$

where q_i is the component of the vector of generalized coordinates $\mathbf{q} = [r, \nu, \theta, x, y]$, Q_i is the generalized forces

$$\begin{aligned} &Q_r = F_x\cos\theta - F_y\sin\theta + P_x, \qquad Q_\nu = F_x r\sin\theta + F_y r\cos\theta - P_x y + P_y(r+x) + L_z, \\ &Q_\theta = L_z, \qquad Q_x = P_x, \qquad Q_y = P_y. \end{aligned} \quad (4)$$

Substitution of expressions (1) and (4) into equations (3) and simplifications give

$$\ddot{r} = \dot{\nu}^2 r - \frac{\mu}{r^2} + \frac{F_x\cos\theta - F_y\sin\theta}{m_B} + \frac{3\mu(3I_x\cos^2\theta + 3I_y\sin^2\theta - I_x - I_y + 2I_z)}{2m_B r^4}, \quad (5)$$

$$\ddot{\nu} = -\frac{2\dot{\nu}\dot{r}}{r} + \frac{F_x\sin\theta + F_y\cos\theta}{m_B r} - \frac{3\mu(I_x - I_y)\sin\theta\cos\theta}{m_B r^5}, \quad (6)$$

$$\ddot{\theta} = \frac{L_z}{I_z} + \frac{2\dot{\nu}\dot{r}}{r} - \frac{F_x\sin\theta + F_y\cos\theta}{m_B r} + \frac{3\mu(I_x - I_y)\sin\theta\cos\theta}{r^3}\left(\frac{1}{m_B r^2} + \frac{1}{I_z}\right), \quad (7)$$

$$\ddot{x} = \ddot{\nu}y - \ddot{r} + \dot{\nu}^2(r+x) + 2\dot{\nu}\dot{y} + \frac{P_x}{m_A} - \frac{\mu(r+x)}{r_A^3}, \quad (8)$$

$$\ddot{y} = \dot{\nu}^2 y - \ddot{\nu}(r+x) - 2\dot{\nu}(\dot{r}+\dot{x}) + \frac{P_y}{m_A} - \frac{\mu y}{r_A^3}. \quad (9)$$

In the general case, ion beam forces F_x, F_y and torque L_z depend on the relative position of the active spacecraft x, y, the direction of the axis of the ion beam, and the orientation of the space debris, given by the angle θ. If the control system of the spacecraft maintains its constant relative position, then $x = const$, $y = const$, and the motion of the space debris is described by three equations (5)-(7). Since $1/r << 1$ and the magnitude of the ion forces is about 10 mN, discarding the small terms in these equations gives

$$\ddot{r} = \frac{c^2}{r^3} - \frac{\mu}{r^2} + \frac{F_x\cos\theta - F_y\sin\theta}{m_B}, \quad (10)$$

$$\dot{c} = \frac{r(F_x\sin\theta + F_y\cos\theta)}{m_B}, \quad (11)$$

$$\ddot{\theta} = \frac{L_z}{I_z} + \frac{2c\dot{r}}{r^3} + \frac{3\mu(I_x - I_y)\sin\theta\cos\theta}{I_z r^3}, \quad (12)$$

where $c = \dot{\nu}r^2$ is the angular momentum.

Consider the motion of the space debris object relative to its center of mass. It is assumed that the object's center of mass moves along a Kepler orbit, which focal parameter $p = c^2\mu^{-1}$ and eccentricity e change slowly. In this case the length of the position vector is defined as $r = p(1+e\cos\nu)^{-1}$. Let us fix the values of focal parameter and eccentricity, and choose the true anomaly angle ν as the time dependent variable. A prime symbol denotes a derivative with respect to the true anomaly angle. The equation of angular oscillations of space debris (12) can be rewritten in the form

$$\theta'' = \frac{L_z}{I_z}\frac{p^4}{c^2(1+e\cos\nu)^4} + \frac{2e(\theta'+1)\sin\nu}{1+e\cos\nu} + \frac{3(I_x - I_y)\sin 2\theta}{2I_z(1+e\cos\nu)}. \quad (13)$$

For the case of small eccentricity $e << 1$ equation (13) can be expanded in a Macloren series. Discarding nonlinear terms, we obtain the following approximate equation:

$$\theta'' = \frac{L_z c^6}{I_z \mu^4} + \frac{3(I_x - I_y)\sin 2\theta}{2I_z} + e\left(2(\theta' + 1)\sin v - \frac{4 L_z c^6 \cos v}{\mu^4 I_z} - \frac{3(I_x - I_y)\sin 2\theta \cos v}{2I_z} \right). \quad (14)$$

The process of obtaining the ion beam torque L_z is described in the paper [10]. It is assumed that the active spacecraft maintains a constant distance to the center of mass of the space debris object, and the axis of the ion beam passes through it center. After numerically calculating this torque, it can be represented as a Fourier series

$$L_z = L_z^{\max}\left(a_0 + \sum_{j=1}^{k} (a_j \cos j\theta + b_j \sin j\theta) \right), \quad (15)$$

where $L_z^{\max}$ is maximum absolute value of the ion beam torque, a_j, b_j are dimensionless Fourier coefficients. Equation (14) can be rewritten in the following form, taking into account (15)

$$\begin{gathered} \theta'' - A\left(a_0 + \sum_{j=1}^{k} (a_j \cos j\theta + b_j \sin j\theta) \right) - B\sin 2\theta = \\ = e\left(2(\theta' + 1)\sin v - \frac{4 L_z c^6 \cos v}{\mu^4 I_z} - \frac{3(I_x - I_y)\sin 2\theta \cos v}{2I_z} \right), \end{gathered} \quad (16)$$

where $A = \frac{L_z^{\max} c^6}{I_z \mu^4}$, $B = \frac{3(I_x - I_y)}{2I_z}$. Equation (16) describes the perturbed motion of a space debris object under the action of gravitational and ion beam moments. The small perturbation in the right-hand side of the equation is periodic and, if the unperturbed system ($e = 0$) has hyperbolic singular points, creates the prerequisites for chaos. The type and arrangement of the singular points of the unperturbed equation

$$\theta'' - A\left(a_0 + \sum_{j=1}^{k} (a_j \cos j\theta + b_j \sin j\theta) \right) - B\sin 2\theta = 0 \quad (17)$$

depends on the ratio γ of the coefficients A and B:

$$\gamma = \frac{A}{B} = \frac{L_z^{\max} c^6}{I_z \mu^4} = \frac{2 L_z^{\max} p^3}{3\mu (I_x - I_y)}. \quad (18)$$

and the coefficients of the expansion in the Fourier series a_j and b_j. The parameter characterizes the relationship between the ion and the gravitational moments. As the height increases, the influence of the ion beam moment will increase in comparison with the influence of the gravitational moment. It can be seen that this parameter is proportional to the space debris orbit's focal parameter p, and it will change as the altitude of the orbit changes during space debris removal mission.

It is very difficult to analyze the phase portrait of the unperturbed equation (17) in general case, since the coefficients of equation (17) depend on many parameters, including the mass, shape and layout of the space debris object, the parameters of the ion beam, its direction and the distance between the active spacecraft and the space debris object. Perform further analysis for a specific space debris object. The upper stage of the Arian rocket is taken as a sample.

3. Results of numerical simulations

3.1. Mechanical system parameters

Consider the orbital motion of a cylindrical body close in shape and mass to the Ariane 4 H10 stage [18]. The mass of the space debris object is $m_B = 2150\,\text{kg}$, its length is 7m, its radius is 1.3 m. The center of mass lies on the axis of symmetry and is located at a distance of 1.75 m from the bottom cover. The active spacecraft has a mass $m_A = 1500\,\text{kg}$ and it is located at a distance of 15 m from space debris ($x = 0$, $y = 15\,\mathrm{m}$). The spacecraft creates ion beam with following parameters: the mass of the particle is $2.18 \cdot 10^{-25}\,\mathrm{kg}$, the plasma density is $2.6 \cdot 10^{16}\,\mathrm{m}^{-3}$, ion flux velocity is $38000\,\mathrm{m/s}$, divergence angle of the ion beam is $15°$. To calculate the effect of an ion beam on a space debris object, the methodology described in the papers [9, 10] and implemented in the MATLAB was used by the authors. Table 1 contains the Fourier series coefficients for various positions of the center of mass. The distance from the upper base of the cylinder to the center of mass is denoted by Δ in the table. The moments of inertia for various cases (table 1) are $I_x = 1817\,\mathrm{kg \cdot m^2}$, case 1: $I_y = I_z = 4390\,\mathrm{kg \cdot m^2}$; case 2: $I_y = I_z = 10974\,\mathrm{kg \cdot m^2}$; case3: $I_y = I_z = 30727\,\mathrm{kg \cdot m^2}$.

Table 1. The expansion coefficients of the ion beam torque in a Fourier series (15) for various options for the center of mass position.

	Case 1 $\Delta = 3.5\,\mathrm{m}$ $L_z^{max} = 0.016\ \mathrm{N \cdot m}$		Case 2 $\Delta = 2.625\,\mathrm{m}$ $L_z^{max} = 0.0234\,\mathrm{N \cdot m}$		Case 3 $\Delta = 1.75\,\mathrm{m}$ $L_z^{max} = 0.0299\,\mathrm{N \cdot m}$	
j	a_j	b_j	a_j	b_j	a_j	b_j
0	0	0	0.0027	0	0.0036	0
1	0	0.0045	0.3159	-0.0102	0.5711	-0.0096
2	0	0.7174	-0.0035	0.4288	-0.0050	0.2599
3	0	0.0265	-0.1459	0.0167	-0.1725	0.0100
4	0	-0.4249	-0.0018	-0.3034	-0.0027	-0.2269
5	0	-0.0249	0.0886	-0.0156	0.1243	-0.0090
6	0	0.1728	0.0064	0.1353	0.0079	0.1280
7	0	0.0124	-0.0376	0.0089	-0.0545	0.0081
8	0	-0.1083	-0.0050	-0.0825	-0.0074	-0.0918
9	0	-0.0040	0.0174	-0.0039	0.0423	-0.0057
10	0	0.0589	0.0023	0.0411	0.0046	0.0455

3.2. Bifurcation diagram

For the unperturbed equation (17), let us construct a bifurcation diagrams in which the location and type of singular points depending on the value of the parameter γ will be shown. Figure 2 shows three bifurcation diagrams constructed for the cases shown in Table 1. The solid line shows unstable equilibrium positions, and the dashed line indicates stable ones. It is seen that the position of the center of mass has a significant effect on the location and type of equilibrium positions. In the ideal case, when the center of mass is at the intersection of the axis and the plane of symmetry (case 1), the position $\theta = 0$ is unstable and positions $\theta = \pm\pi/2$ are stable when the parameter $\gamma << -1$. In this case, the ion beam moment has a decisive influence on the motion of the space debris. As parameter γ increases with $\gamma = -5.04$, bifurcation occurs and new stable and unstable singular points appear in the vicinity of an unstable equilibrium position. Starting from this value of the parameter, the gravitational moment begins to have a noticeable effect on the motion of the space debris object. When $\gamma = -4.17$, the next bifurcation occurs and the position $\theta = 0$ becomes stable due to the increased influence of the gravitational moment. Positions $\theta = \pm\pi/2$ always stay stable.

With a shift of the center of mass closer to the upper edge of the cylinder, the picture changes significantly. Position $\theta = \pi/2$ remains stable. A singular point in the vicinity of zero disappears. It is shown in the [10] that transportation is the most efficient when the cylindrical space debris is in position $\theta = 0$, that is, the axis of symmetry is perpendicular to the axis of the stream. According to bifurcation diagrams, in all three cases considered there is a stable position of equilibrium in a neighborhood of position $\theta = 0$ for small in absolute values of parameter γ . That is, when the height is relatively small and the gravitational moment has a dominant effect. At high altitudes, oscillations occur near positions $\theta = \pm\pi / 2$. This means that for the effective transportation of space debris, additional efforts are required to stabilize it in position $\theta = 0$.

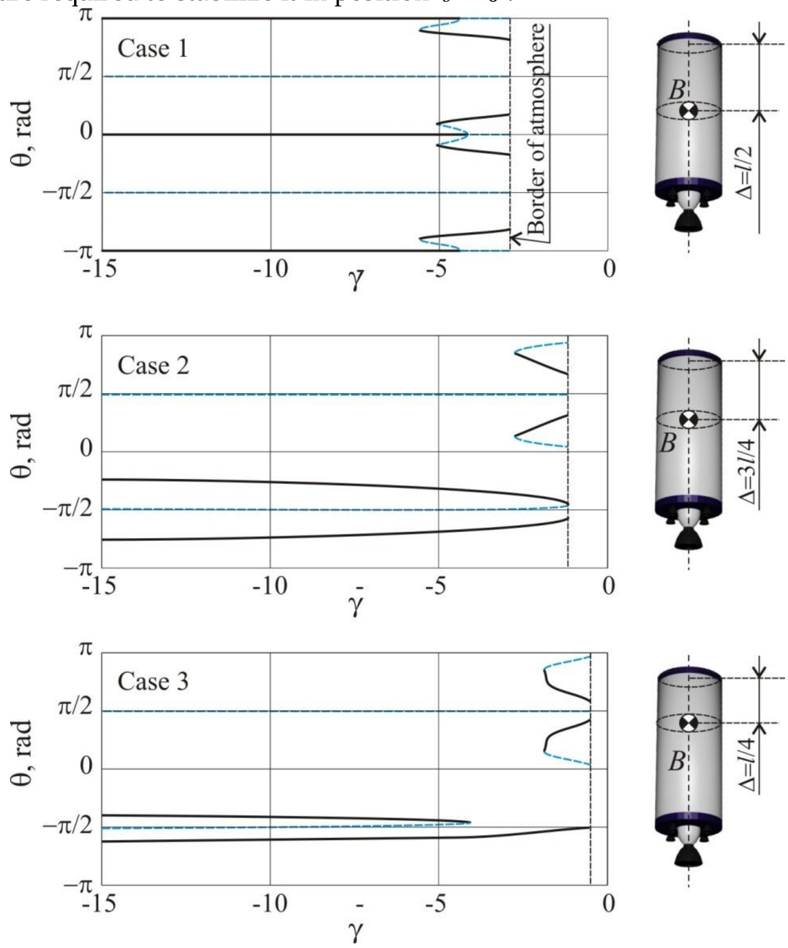

Figure 2. Bifurcation diagrams for the cases shown in table 1.

3.3. Chaotic motion

In order to show that there is chaos in the considered mechanical system, let us construct Poincare sections for different values of the eccentricity of the orbit. As an example, case 3 from table 1 is selected when $\gamma = -1$. Figure 3 shows a phase portrait of the unperturbed equation (17). Three stable singular points of the center type and three unstable points of the saddle type are observed in the phase portrait. In the case of perturbed motion, when the eccentricity is not equal to zero ($e \neq 0$), a cloud of points is observed in the vicinity of the separatrices of the internal vibrational region (figures 4), which indicates the presence of chaotic motion. Inside this chaotic region there is a non-periodic trajectory that does not intersect anywhere. Calculations show that with an increase in eccentricity, the thickness of the chaotic layer increases. Outside the clearly visible oscillatory region in Figure 4, a region of unbounded non-periodic trajectories is observed. Hit of the imaging phase space point in this area will cause the object of space debris to unwind and its angular velocity will gradually increase.

The chaotic nature of the trajectory can be confirmed by calculating the spectrum of Lyapunov exponents for it. As a starting point, a point inside the chaotic layer $\theta_0 = 1.1\,\text{rad}$, $\theta_0' = 0$ is selected.. For the trajectory passing through this point, the spectrum of Lyapunov exponents can be calculated in expanded phase space $\{\theta, \theta', \nu\}$ using the known procedure [19]. The following values were obtained: $\Lambda = [0.100,\ 0.001,\ -0.201]$. It can be said that the Lyapunov spectrum includes a positive, zero, and negative exponents. Such a set of evidence of chaotic trajectories.

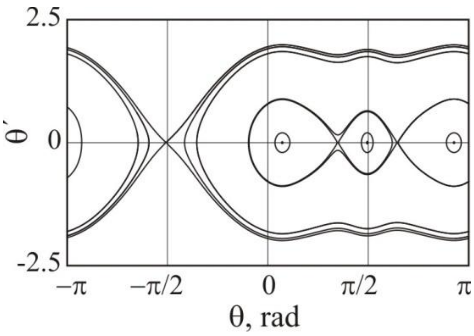

Figure 3. Phase portrait of the unperturbed equation (17) for case 3 from table 1.

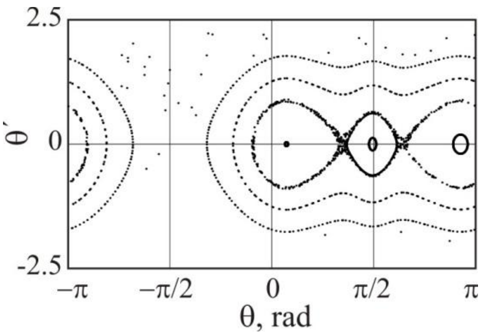

Figure 4. Poincare sections for $e = 0.001$.

4. Conclusion

The angular motion of a passive space debris object of cylindrical shape relative to the center of mass during its contactless transport by an ion beam was considered. A mathematical model was constructed using second-order Lagrange equations. An assumption was made that the center of mass moves in the Kepler orbit, and the angle of the true anomaly was taken as a new independent variable. Then, a linearized equation describes the oscillations of the space debris object for the case of small eccentricity was written. Using this equation, the influence of the position of the center of mass on the object oscillations was studied. A dimensionless parameter that characterizes the ratio of the gravitational and ionic effects on the space debris was introduced. Bifurcation diagrams describing the location and type of singular points of the system depending on the value of this parameter were constructed for three different positions of the space debris center of mass. Analysis of the diagrams showed that the position when the axis of the cylindrical space debris is oriented along the local vertical is stable at low altitudes. At high altitude, where the influence of the gravitational moment is small compared with the moment of the ion beam, additional efforts are required to stabilize the object in this position. Using Poincare sections and the Lyapunov exponent spectrum, it was shown that the motion of a space debris object can be chaotic. The chaotic layer is observed at the Poincare sections in the vicinity of the separatrices of the unperturbed system. The thickness of this layer increases with an increase in eccentricity. Chaotization motion can occur in an uncontrolled change of the amplitude of oscillation of the space debris object during its contactless transportation. The results of this work can be useful in the development of active space debris removal systems based on ion beam contactless interaction.

5. Acknowledgments

This study was supported by the Russian Foundation for Basic Research (RFBR 18-01-00215-A).

6. References

[1] Shan, M. Review and comparison of active space debris capturing and removal methods / M. Shan, J. Guo, E. Gill // Prog. Aerosp. Sci. – 2016. – Vol. 80. – P. 18-32.
[2] Zemoura, M. Removal targets' classification: How time considerations modify the definition of the index / M. Zemoura, T. Hanada, S. Kawamoto // Adv. Space Res. – 2017. – Vol. 60(6). – P. 1163-1187.
[3] Mark, C.P. Review of active space debris removal methods / C.P. Mark, S. Kamath // Space Policy. – 2019. – Vol. 47. – P. 194-206.
[4] Shuvalov, V.A. Physical simulation of the long-term dynamic action of a plasma beam on a space debris object / V.A. Shuvalov, N.B. Gorev, N.A. Tokmak, G.S. Kochubei // Acta Astronaut. – 2017. – Vol. 132. – P. 97-102.
[5] Cichocki, F. Spacecraft-plasma-debris interaction in an ion beam shepherd mission / F. Cichocki, M. Merino, E. Ahedo // Acta Astronaut. – 2018. – Vol. 146. – P. 216-227.

[6] Dominguez-Vazquez, A. Axisymmetric plasma plume characterization with 2D and 3D particle codes / A. Dominguez-Vazquez, F. Cichocki, M. Merino, P. Fajardo, E. Ahedo // Plasma Sources Sci. T. – 2018. – Vol. 27(10). – P. 1-22.
[7] Taccogna, F. Latest progress in Hall thrusters plasma modelling / F. Taccogna, L. Garrigues // Rev. Mod. Plasma Phys. – 2019. – Vol. 3(1). – P. 1-12.
[8] Cichocki, F. Modeling and Simulation of EP Plasma Plume Expansion into Vacuum / F. Cichocki, M. Merino, E. Ahedo // 50th AIAA/ASME/SAE/ASEE Joint Propulsion Conference, AIAA Paper. – 2014. – Vol. 3828. – P. 5008-5024.
[9] Alpatov, A. Determination of the force transmitted by an ion thruster plasma plume to an orbital object / A. Alpatov, F. Cichocki, A. Fokov, S. Khoroshylov, M. Merino, A. Zakrzhevskii // Acta Astronaut. – 2016. – Vol. 119. – P. 241-251.
[10] Aslanov, V.S. Attitude motion of cylindrical space debris during its removal by ion beam / V.S. Aslanov, A.S. Ledkov // Math. Probl. Eng. – 2017. – Vol. 2017. – P. 1-7.
[11] Bombardelli, C. Ion beam shepherd for contactless space debris removal / C. Bombardelli, J. Pelaez // J. Guid. Control Dynam. – 2011. – Vol. 34(3). – P. 916-920.
[12] Cichocki, F. Electric propulsion subsystem optimization for "Ion Beam Shepherd" missions / F. Cichocki, M. Merino, E. Ahedo, M. Smirnova, A. Mingo, M. Dobkevicius // J. Propul. Power. – 2017. – Vol. 33(2). – P. 370-378.
[13] Alpatov, A. Relative control of an ion beam shepherd satellite using the impulse compensation thruster / A. Alpatov, S. Khoroshylov, C. Bombardelli // Acta Astronaut. – 2018. – Vol. 151. – P. 543-554.
[14] Khoroshylov, S. Out-of-plane relative control of an ion beam shepherd satellite using yaw attitude deviations // Acta Astronaut. – 2019. – Vol. 164. – P. 254-261.
[15] Urrutxua, H. A Preliminary Design Procedure for an Ion-Beam Shepherd Mission / H. Urrutxua, C. Bombardelli, J.M. Hedo // Aerosp. Sci. Technol. – 2019. – Vol. 88. – P. 421-435.
[16] Aslanov, V.S. Space debris attitude control during contactless transportation in planar case / V.S. Aslanov, A.S. Ledkov / J. Guid. Control Dynam, 2020 [Electronic resource]. – Access mode: https://arc.aiaa.org/doi/abs/10.2514/1.G004686 (14.11.2019)
[17] Nakajima, Y. Contactless Space Debris Detumbling: A Database Approach Based on Computational Fluid Dynamics / Y. Nakajima, H. Tani, T. Yamamoto, N. Murakami, S. Mitani, K. Yamanaka // J. Guid. Control Dynam. – 2018. – Vol. 41(9). – P. 1906-1918.
[18] Gomez, N.O. Eddy currents applied to de-tumbling of space debris: Analysis and validation of approximate proposed methods / N.O. Gomez, J.I. Walker // Acta Astronaut. – 2015. – Vol. 114. – P. 34-53.
[19] Skokos, C. The lyapunov characteristic exponents and their computation // Dynam. Small Solar Syst. Bodies and Exoplanets – Springer: Berlin, Heidelberg, 2010. – P. 63-135.